



Analysis of the adhesive damage for different shapes and types patch's in corroded plates with an inclined crack

Hayet Benzineb, Mohamed Berrahou, Mohamed Serier

University of Relizane, GIDD Laboratory, Relizane, Algeria

hayetbenzineb7@gmail.com, Mohamed.berrahou@univ-relizane.dz, moha_serier@yahoo.fr

ABSTRACT. In this study, the finite element method is used to analyze the effect of corrosion and the behavior of inclined cracks of an aluminum plate Al 2024 -T3 under thermomechanical loading. The effects of the inclination of the crack and the effect of temperature for different types and shapes of adhesives are highlighted. The results obtained show the increase of the crack inclination leads to a decrease of the damaged area and the damaged area ratio of the adhesive. In addition, the ratio D_R increases with increasing temperature variation ΔT . The best performing patch shape that gave interesting results during this analysis is the circular and for type the Boron/epoxy is the best.

KEYWORDS. Composite; Temperature Variation; Stress Intensity Factor; Damaged Zone Ratio; Finite Element Method (FEM); Thermomechanical Loading.



Citation: Benzineb, H., Berrahou, M., Serier, M., Analysis of the adhesive damage for different shapes and types patches in Aircraft Structures corroded with an inclined crack, *Frattura ed Integrità Strutturale*, 60 (2022) 331-345.

Received: 14.12.2021

Accepted: 21.02.2022

Online first: 02.03.2022

Published: 01.04.2022

Copyright: © 2022 This is an open access article under the terms of the CC-BY 4.0, which permits unrestricted use, distribution, and reproduction in any medium, provided the original author and source are credited.

INTRODUCTION

The industrial development and technological progress depend on the use of advanced materials with good mechanical properties, among these materials is aluminum. Taking into account modern industrial requirements, there are several researches to develop this material and increase its efficiency in order to reduce its cost price. Aluminum is an excellent metal, and this is due to its effectiveness in resisting corrosion. There are several techniques developed to solve the corrosion problem by adding inhibitors or application of paint and surface treatment. Knowing the properties of the adhesive plays a fundamental role in predicting its targeted damage. Many authors such as Berrahou [1-6] have worked on the effect of corrosion on the damaged area of the adhesive FM73 of a plate repaired with composite materials by applying the damaged zone theory. There are several works on the study of only corroded plates without cracks, and others on corroded plates with horizontal cracks under mechanical loading.

The use of the damaged area theory in recent times has been widely spread due to its discretionary advantages to avoid failure of the compound used to repair cracks and also to avoid the corrosion. Recently, several papers describing the damage zone theory of the FM73 adhesive were publishing. The adhesive damage and failure to repair the adhesive structure are estimated using modified damage area theory [7-14]. Mokadem and his colleague Berrahou [6] analyzed the effect of the crack inclination on the performance of the composite and from the results they concluded that increasing



the crack inclination leads to an increase in the damaged area ratio (D_R) and also leads in turn to a decrease of the values of the stress intensity factor in mode I (K_I).

In this work we have studied the effect of the Thermomechanical Loading on the change of the stress intensity factor, The Stress intensity factor (SIF) at the crack front was extracted by using the virtual crack closure technique (VCCT). This technique is based on the energy balance proposed by Irwin. The idea presented by Rybicki and Kanninen [15] is based on the calculation of the energy release rate, using Irwin assumption that the energy released in the process of crack expansion is equal to work required to close the crack to its original state. The calculations are performed with the ABAQUS numerical code using Cohesive Zone Modelling (CZM) and the Xtended finite element method (XFEM). Many studies that dealt with the analysis of the application of VCCT, XFEM and ZCM methods[16-18]. Researchers J. Jokinen and M. Kanerva demonstrated the effects of free-edge stress concentrations and surface separation prior to nodal release on the VCCT and ZCM model [16]. Billali et al performed calculations using ABAQUS numerical code using CZM coherence elements for patch separation and XFEM technique for plate fracture [18].

The finite element method has been used to develop the repair method, and study the spread of cracks in aluminum plates and their treatment by the technique of composite patches [19, 20]. Experimentally, no researcher has studied the repair of cracked plates using the Glass-epoxy composite because of its characteristics such as its low efficiency, the high coefficient of expansion, the ease of its preparation compared to those Boron-epoxy and Graphite-epoxy.

Numerical analysis was studied by the three-dimensional finite element method of repairing aluminum structure Al 2024 T-3 with bonded composite. The effect of the corrosion on the damage of the adhesive (FM73) in the length of inclined crack located on the left side is presented, to evaluate the variation in the damaged area ratio of the adhesive (D_R). The major issue is the damaged area of the adhesive to the standard ($D_R < 0.247$), and the protection of aluminum alloys in order to provide the system with properties in the presence of corrosion and thus reinforce the corrosion resistance properties. The effects of crack size, mechanical properties of the composite patch, its geometric shape and thermal loading are demonstrated on the variation of the damaged area of the adhesive. The variation of the stress intensity factor at the tip of the crack repaired by a simple patch was studied in order to observe the behavior of the damaged area. Our work consists to improve the repair performance of a cracked and corroded plate subjected to thermomechanical loadings in mixed modes (I and II).

Materials	Al 2024-T3	Adhesive	Boron/epoxy	Glass/epoxy	Graphite/epoxy
Height (mm)	254	see fig.2	see fig.2	see fig.2	see fig.2
Width (mm)	254	see fig.2	see fig.2	see fig.2	see fig.2
Thickness (mm)	5	0.15	1.5	1.5	1.5
E1 (GPa)	72		200	50	127.5
E2 (GPa)			19.6	25	9.00
E3 (GPa)			19.6	25	4.80
ν_{12}	0.33	0.32	0.3	0.21	0.342
ν_{13}			0.28	0.21	0.342
ν_{23}			0.28	0.21	0.38
G12 (GPa)		4.2	7.2	7.2	4.8
G13 (GPa)			5.5	5.5	4.8
G23 (GPa)			5.5	5.5	2.55
$\alpha_{12}(10^{-6} \text{ C}^\circ)$	22.5		4.5	5.5	-1.2
$\alpha_{13}(10^{-6} \text{ C}^\circ)$			23	15	34
$\alpha_{23}(10^{-6} \text{ C}^\circ)$			23	15	34
Dimensions			Mechanical and Thermal Properties		

Table 1: Mechanical, thermal and dimensional properties of different materials.

GEOMETRICAL MODELS

To facilitate the understanding of the problem addressed in this article, in Tab. 1, all the mechanical and thermal properties of the materials used in the structure are indicated . To be more realistic, an aluminum plate having a corrosion of random shape, is subjected to the influence of a thermal loading, in situations close to reality with temperature variations: normal

$T=20^{\circ}\text{C}$ ($\Delta T=0^{\circ}\text{C}$) and very hot $T=100^{\circ}\text{C}$ ($\Delta T=80^{\circ}\text{C}$). Knowing that the adhesive conforms to the shape of the patch used during the repair. As for the shapes of the adhesive matching the shape of the patch, we took several shapes to find the optimal shape (Rectangular, trapezoidal and circular). These shapes and their dimensions are shown in fig. 1.

In order to analyze the effect of the patch shape, three shapes were chosen in this study: rectangular, trapezoidal and circular, having the same area $A \approx 39000\text{mm}^2$. The dimensions of the materials related to this work (aluminum plate, composite patch and adhesive) are shown in Fig. 1. The patch is glued using FM 73 adhesive with a thickness = 0.15 mm. The plate is subjected to a thermal loading which varies in the interval T (0°C - 100°C) and a uniaxial tensile load of amplitude $\sigma = 200\text{MPa}$. The damaged area is estimate from modern techniques to know the value at which the adhesive rupture occurs. In our work, the evaluation of the breaking stress of the FM 73 adhesive is calculated from the curve in Fig. 2.

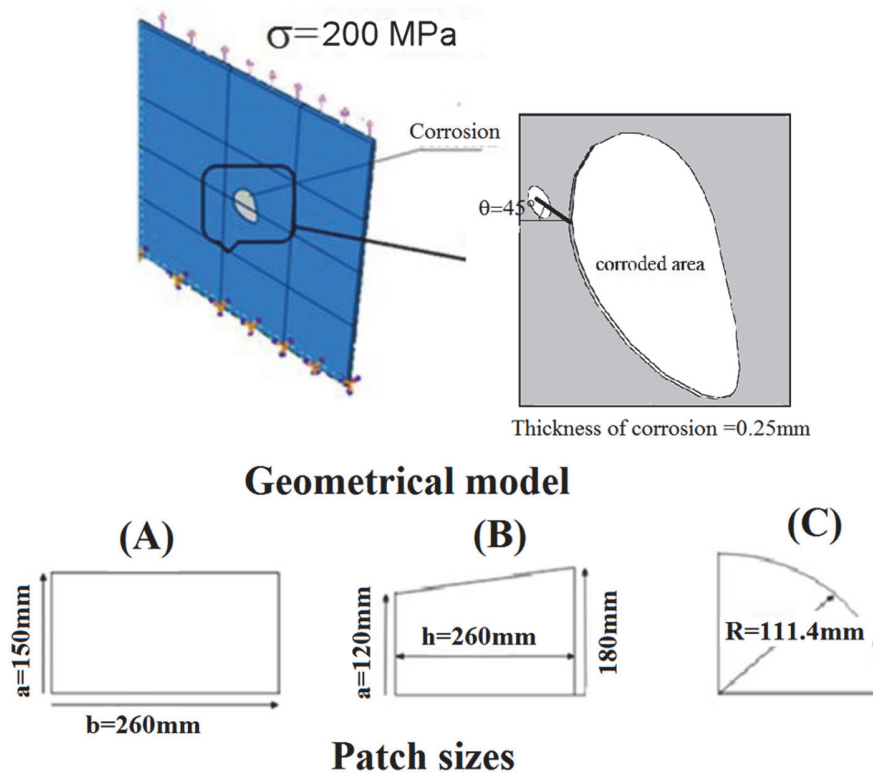


Figure 1: Geometrical model of plate and patch sizes of (A) Rectangular shape, (B) Trapezoidal shape and (C) Circular shape.

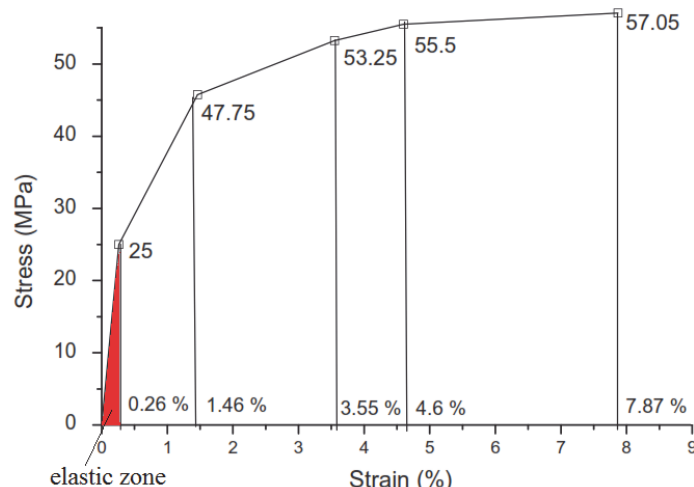


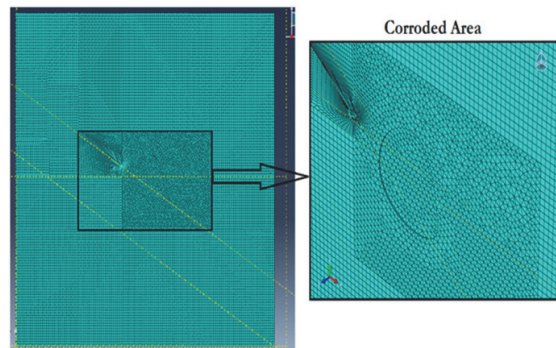
Figure 2: Stress-strain curve of the adhesive FM 73.



NOMINAL FINITE ELEMENT MODELING

The study of this work was carried out by the three-dimensional finite element method using the calculation code ABAQUS [21]. The finite element model is applied for the three parts of the structure, a plate with a corrosion of random shape, the adhesive, and the composite (patch). The number of elements layers in the thickness direction is as follows four for the aluminum plate, one for the adhesive and two for the composite patch. The mesh was refined near the corrosion zone with an element dimension of 0.05 mm using at least twenty of these fine elements around the corrosion. Fig. 3 shows the overall mesh of the structure, the mesh refinement in the corrosion zone. Moreover, the mesh of the structure (plate, adhesive and patch in composite) is shown in Fig. 3.

The total number of elements for the repaired structure depends on the patch shape. The total number of elements is shown in Tab. 2.



Refined mesh of plate near the corrosion

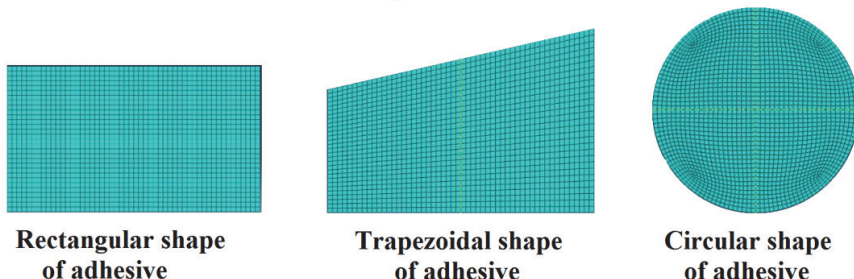


Figure 3: Mesh of the plate near corrosion, and typical finite element (FE) for a global model.

The different components of the analyzed structure	Numbers of elements	Sizes of elements
Aluminum 2024-T3	49646	5mm
corrosion	2300	0.25mm
FM-73 Adhesive type	2470	0.15mm
Composite Patch	9880	1.5mm

Table 2: Number of finite elements of the structure.

RESULTS AND DISCUSSIONS

The Von Mises Failure criterion was introduced by Von Mises (1913) and has been used since as one of the most reliable failure criteria for engineering materials. It relies on the second deviatoric invariant and the effective average stress. Assuming a triaxial test condition where $\sigma_1 > \sigma_2 = \sigma_3$.

$$\sqrt{J_2} = 1/3(\sigma_1 - \sigma_3) \quad (1)$$

The effective average stress can be expressed by the following equation:

$$\sigma_m - P_0 = 1/3(\sigma_1 + 2\sigma_3) - P_0 \quad (2)$$

where P_0 formation pore pressure and the effective average stress is defined as the average stress minus the pore pressure. In the Von Mises shear criterion, the second deviatoric invariant is plotted against the effective average stress for various axial loads σ_1 and confining pressures σ_3 . The resulting curve, known as the failure curve, specifies two regions, one below the curve as being safe and stable and the other above the curve as being unstable and failed as shown in Fig. 4.

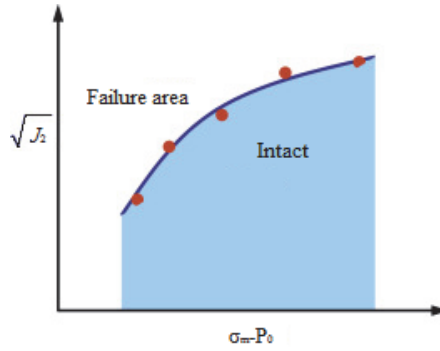


Figure 4: Von Mises failure model from triaxial test data.

The theory's Main assumption of is that the adhesive and crack initiation in the bonded patch occurs after a damaged area develops. Under low amplitude of load, the localized damages arrive at the edges of patch. This damage occurs because the material is locally subjected to strains higher than the ultimate material strain. Under medium load amplitude, the damaged zones grow in size and the concentration of points of the damaged areas increases. As the failure load is reached the damaged area in the adhesive grows to a critical size and the individual components of the damage coalesce and form a crack. Numerically, the damaged area is identified by marking items for which a failure criterion is exceeded. The adhesive tested is a toughened ductile adhesive which is expected to fail in performance. Consequently, the failure criterion used for the cohesive damage of the adhesive layer is the equivalent Von Mises strain criterion:

$$\varepsilon_{equiv} = \frac{1}{\sqrt{2(1+\vartheta)}} X \sqrt{(\varepsilon_{p1} - \varepsilon_{p2})^2 + (\varepsilon_{p2} - \varepsilon_{p3})^2 + (\varepsilon_{p3} - \varepsilon_{p1})^2} \quad (3)$$

where ε_{equiv} is the equivalent stain, ε_{pi} are the plastic strains in the different directions and ϑ the Poisson ratio.

This criterion is satisfied when the maximum principal strain in the material reaches the ultimate principal strain. For each failure criterion an ultimate strain will be defined and the corresponding damage zone size at failure is determined. The damaged area theory is based on the principle that the adhesive joint is assumed to fails when the damaged area reaches a certain critical value. The damaged zone can be determined by either a stress or a strain criterion. Therefore, the adhesive fails to perform its functions when the cohesive failure criterion is satisfied the adhesive joint. Since adhesive failure occurs at the adhesive joint, the adhesive failure criterion for the damaged area should be used. For isotropic materials, failure criteria such as the Von-Mises and Tresca criteria can be used to better understand the adhesive failure. Where Chang-Su Ban proved that the area where the equivalent strain of the adhesive exceeds the ultimate strain of 7.87%. After conducting studies on the FM-73 adhesive they concluded that this adhesive fails when the DR (Damaged area ratio) reaches a percentage exceeding 0.24 which is considered critical [22] see Fig. 4. The value of the damaged area ratio is calculated according to the following relationship:

$$D_R = \text{sum of damaged areas} / \text{total adhesive area} \quad (4)$$

This study was carried out to determine the evolution of the damaged area in the adhesive layer which ensures the adhesion of the composite patch to the cracked plate with randomly shaped corrosion. The area of the damaged zone was calculated for different parameters such as the following effects, patch shapes (rectangular, trapezoidal, and circular), patch types (Boron/epoxy, Graphite/epoxy and Glass/epoxy) and crack inclination under thermo-mechanical loading. The damaged area theory was used to evaluate the progression of damage in the adhesive layer during the analysis. The color of the damaged area can be seen in gray, see Figs. (5, 7, 8 and 9).



Effect of crack inclination on adhesive damage

This analysis presents the variations in the damaged area of the adhesive as a function of the angle of the crack inclination (θ) for a crack length $a=30$ mm of a plate repaired by simple patch. We set the adhesive thickness $e_{ad} = 0.15$ mm and patch thickness $e_{pat} = 1.5$ mm were determined for a composite patch (Boron-epoxy) having a rectangular geometric shape and an applied tensile stress intensity equal to 200MPa. Initially, the crack inclinations were varied $\theta = (15-45-75)^\circ$, after analysis of the different curves obtained from the ratio of the damaged area D_R and the variations in the stress intensity factor K_I , the effects of crack inclination were shown.

Fig. 5 shows the evolution of the damaged zone as a function of the crack inclination for the rectangular shape. In general, it is observed that more the crack inclination increases, the area of the damaged zone decreases. In the case of $\theta = 15^\circ$, we note the presence of a damaged area surrounding the crack as well as small areas at the periphery of the patch. Comparing the results obtained for the inclinations $\theta = 45^\circ$ and $\theta = 75^\circ$ with those of $\theta = 15^\circ$, one notices a decrease in the size of the damaged area progressively in the vicinity of the crack with the increase of the crack inclination (θ).

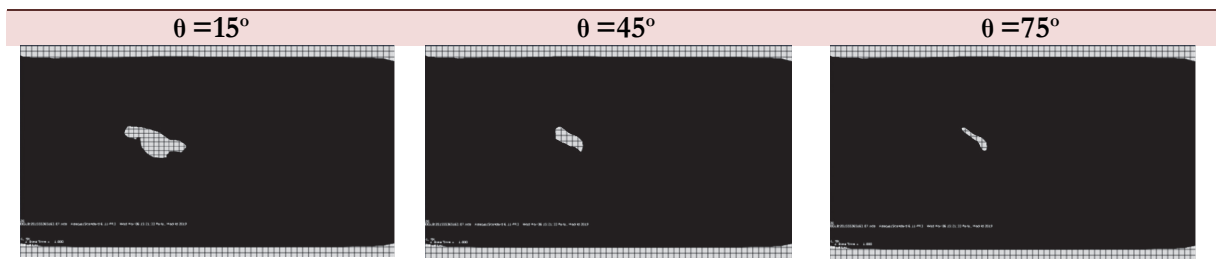


Figure 5: Damaged zone for a patch Boron-epoxy, of rectangular shape for the crack inclination (a) $\theta = 15^\circ$, (b) $\theta = 45^\circ$ and (c) $\theta = 75^\circ$, Adhesive FM 73.

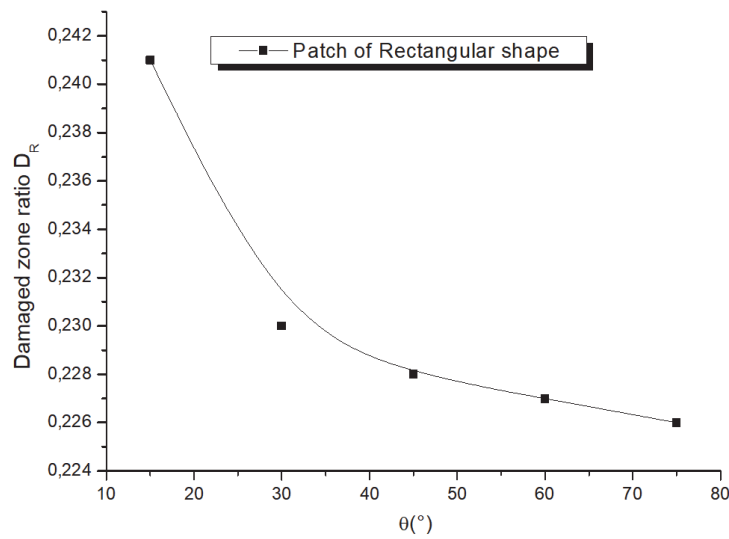


Figure 6: Damaged zone ratio according to the crack inclination.

Fig. 6 shows the variations of the damaged area ratio according to the crack inclination. One observes a strong slope at the start of the graph, which explains the rapid decrease which can reach 33% in the interval of $\theta(15-30)^\circ$, then a gradual slow down to 4% in the damaged area ratio of the adhesive. As a comparison between the values obtained for the inclinations $\theta = 15^\circ$ and $\theta = 30^\circ$ on the one hand and $\theta = 40^\circ$ and $\theta = 75^\circ$ on the other hand, for the first case we have D_R varies from 0.241 to 0.228, the reduction is significant and very rapid, as for the 2nd case one has: $D_R = (0.228-0.226)$ a very insignificant decrease. The values of D_R obtained in this analysis are lower than the critical value D_{Rc} , regardless of the value of the crack inclination. It can be concluded that increasing the crack inclination leads to decrease in the damaged area ratio of the adhesive.

Effect of temperature variation on the damage of the adhesive

This effect is shown in Figs. 7, 8 and 9, that show the variations of the damaged area of the adhesive as a function of the temperature (ΔT) for a crack inclination $\theta = 45^\circ$ repaired by a simple patch. One fixed the thickness of the adhesive $e_{ad} = 0.15$ (mm) and of the patch $e_{pat} = 1.5$ (mm), for different composite patches (Boron-epoxy, Glass-epoxy, Graphite-epoxy) having geometric shapes (rectangular, trapezoidal, circular) and for an applied tensile load equal to $\sigma = 200$ MPa. The temperature variations are included in the interval $T = [20-100]^\circ\text{C}$, ($\Delta T = 0, + 80$) $^\circ\text{C}$.

Boron-epoxy patch

Fig. 7 shows the results which make it possible to follow the evolution of the damaged area as a function of the temperature variation. In general, it is noted that the more the variation in temperature ΔT ($^\circ\text{C}$) increases, the more the surface area of the damaged zone increases. When the variation in temperature ΔT equals 0°C , no damaged zone appears nor at the level of corrosion or crack, only at the edges of the patch. After increasing the temperature, we notice at $\Delta T = 40^\circ\text{C}$ the damaged area develops at the edges in all patch shapes and appears near the crack only in the rectangular shape, but at the maximum temperature $T = 100^\circ\text{C}$ ($\Delta T = 80^\circ\text{C}$) we note that the damaged area includes the edges of the patch and the crack area also in all shapes.

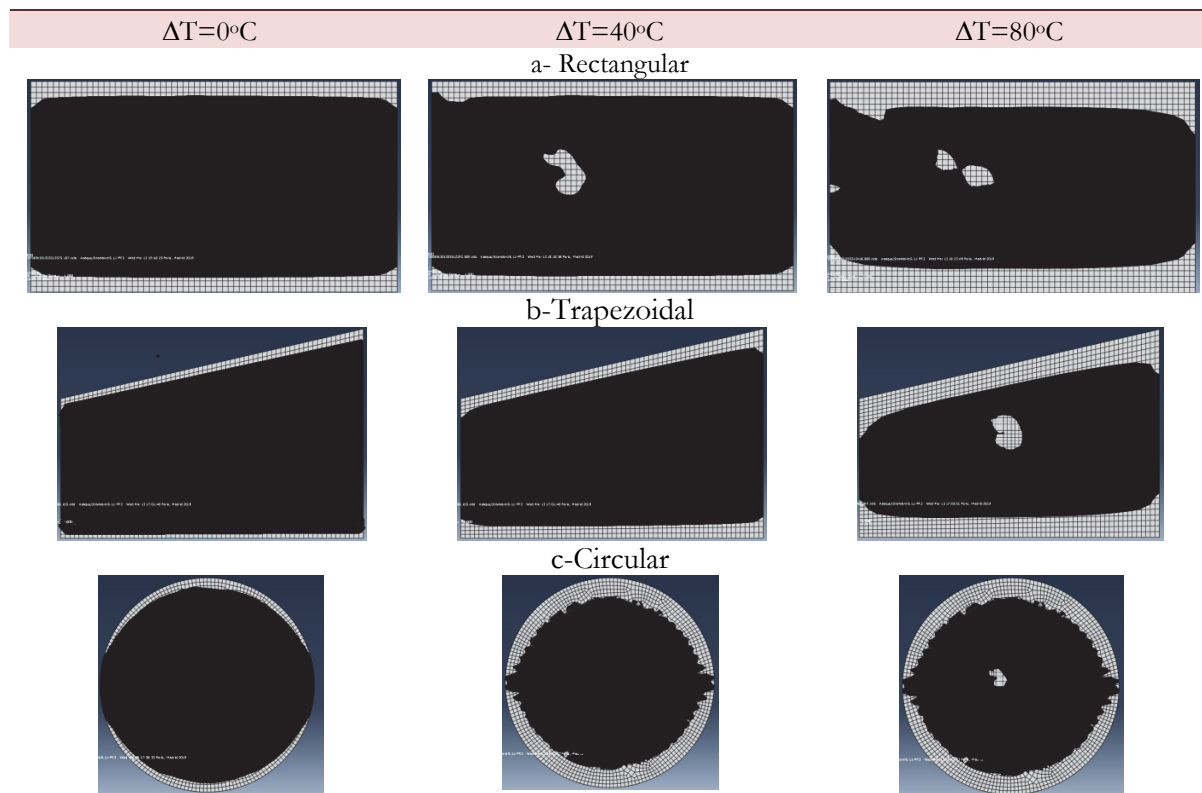


Figure 7: Damaged zone vs the temperature for a Boron-epoxy patch and of type: (a) Rectangular, (b) trapezoidal and (c) circular, for $\theta = 45^\circ$.

Glass-epoxy patch

The evolution of damaged area was presented in Fig. 8 as a function of the temperature variation for a type patch glass/epoxy. We notice that the increase in the temperature variation (ΔT) increases the surface of the damaged area. This damaged area appears around the corroded zone of the plate and at the edges of the patch. The surface of damaged area reaches its maximum for $\Delta T = 80^\circ\text{C}$.

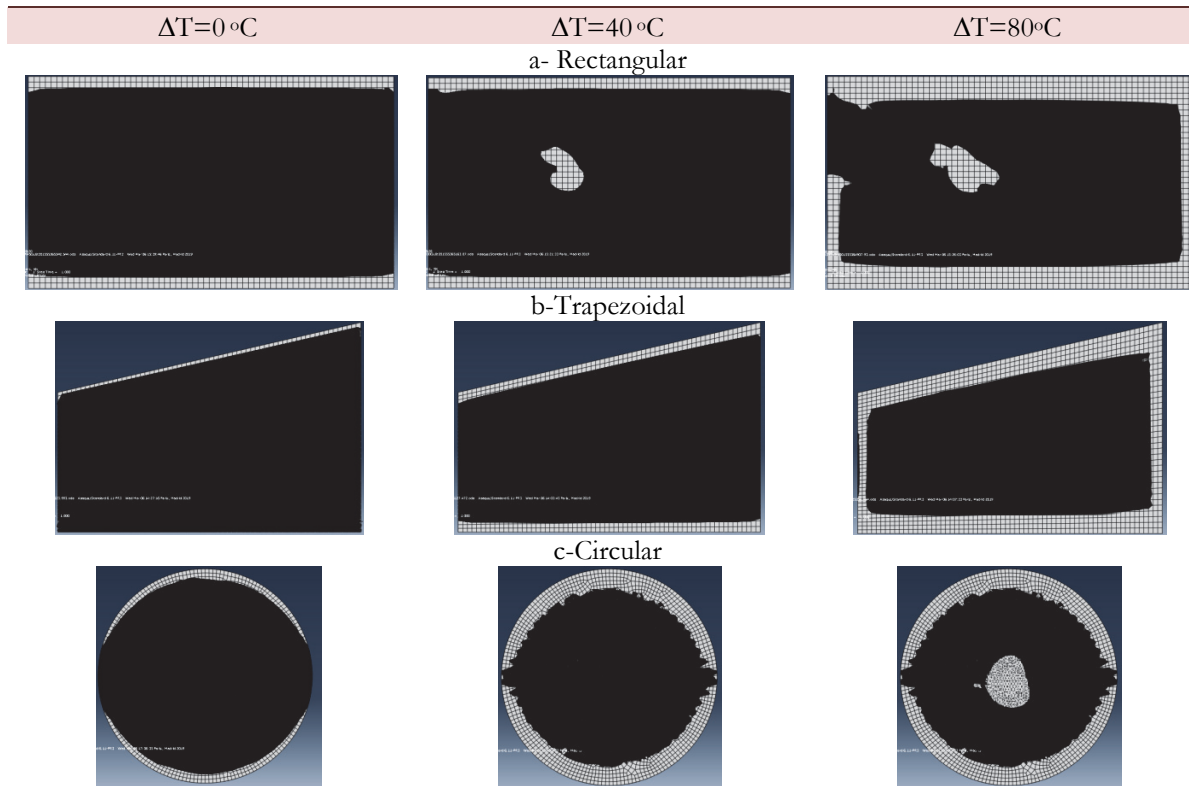


Figure 8: Damaged zone vs the temperature for a Glass-epoxy patch and of type: (a) Rectangular, (b) trapezoidal and (c) circular, for $\theta = 45^\circ$.

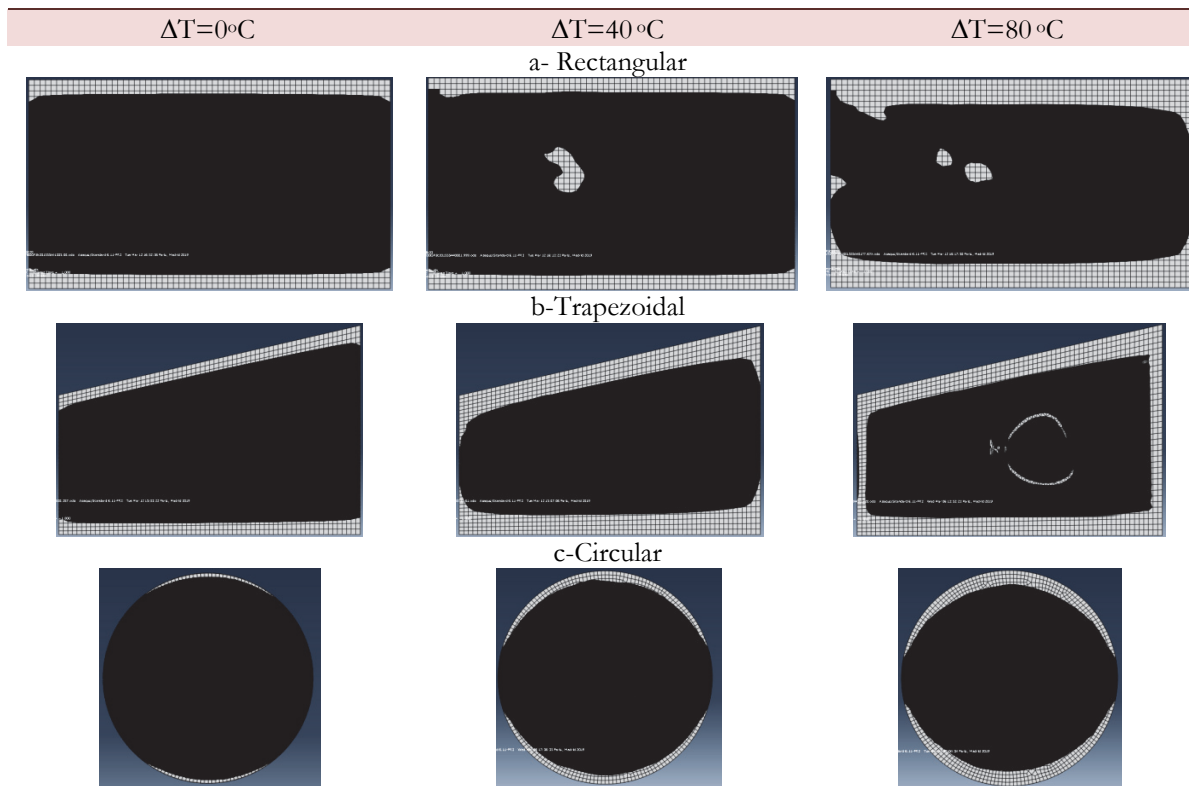


Figure 9: Damaged zone for a Graphite-epoxy patch and of type: (a) Rectangular, (b) trapezoidal and (c) circular, for $\theta = 45^\circ$.

Graphite-epoxy patch

Fig. 9 illustrates the evolution of damaged area of the adhesive according to the temperature variation. It can be seen that an increase in temperature (ΔT) leads to an increase in damaged area. We also notice when the variation in temperature $\Delta T=0^{\circ}\text{C}$ no appearance of damaged area. The surface of the damaged area appears at the edges of the patch and near the corrosion for rectangular and trapezoidal shapes then reaches its maximum for $\Delta T=80^{\circ}\text{C}$.

Variation of the damaged area ratio of the adhesive as a function of temperature

Case of the boron-epoxy patch. Fig. 10 shows the variation of D_R as a function of temperature variation (ΔT) for a Boron/epoxy patch for the three geometric shapes (rectangular, trapezoidal and circular), and for an FM 73 adhesive and with a constant crack inclination $\theta =45^{\circ}$. All curves have the same tendency, because the D_R increases with increasing temperature variation ΔT . As a comparison of the performance across the curves obtained, it can be noted that the circular shape is the most efficient as it gives values of D_R lower than the critical value D_{RC} . This figure also shows that the shapes (rectangular and trapezoidal) are the least performing because the values obtained of D_R exceed the critical value ($D_{RC}=0.2475$) for $T > 70^{\circ}\text{C}$ ($\Delta T > 50^{\circ}\text{C}$). If we compare these two shapes, the rectangular shape is the least performing because it gives higher D_R values than the two other shapes (trapezoidal and circular).

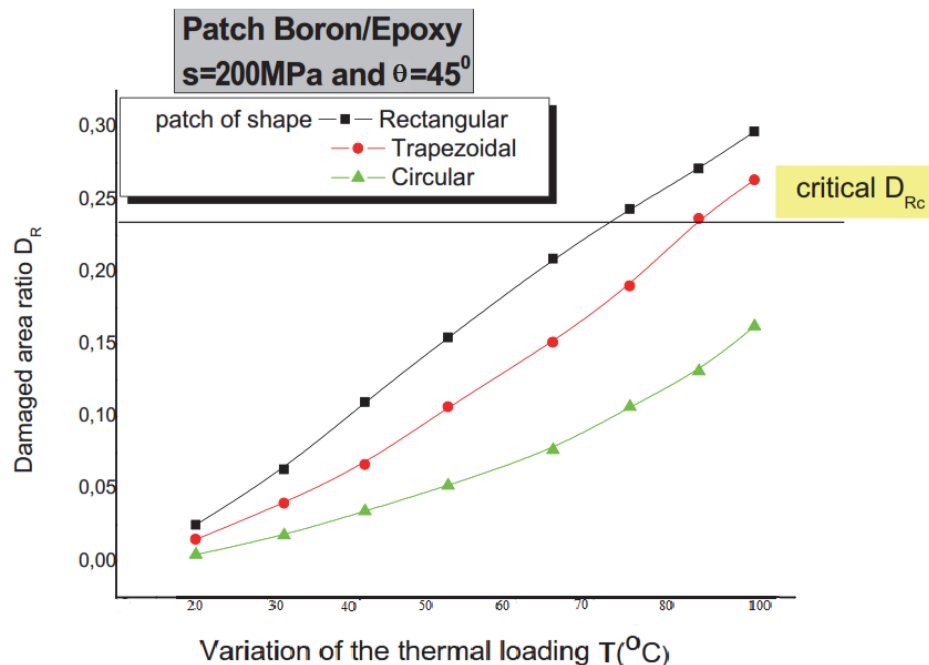
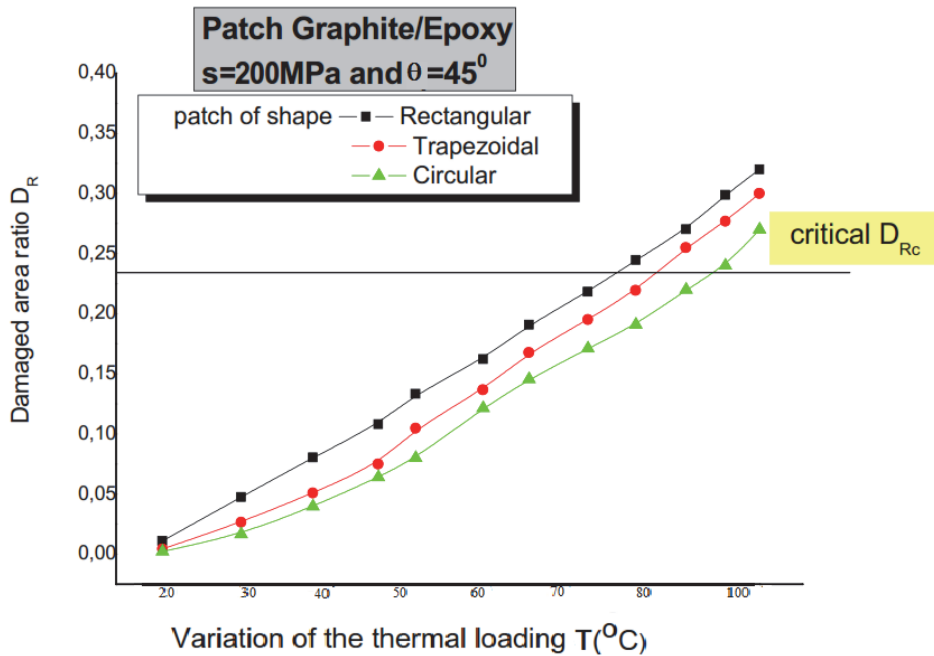
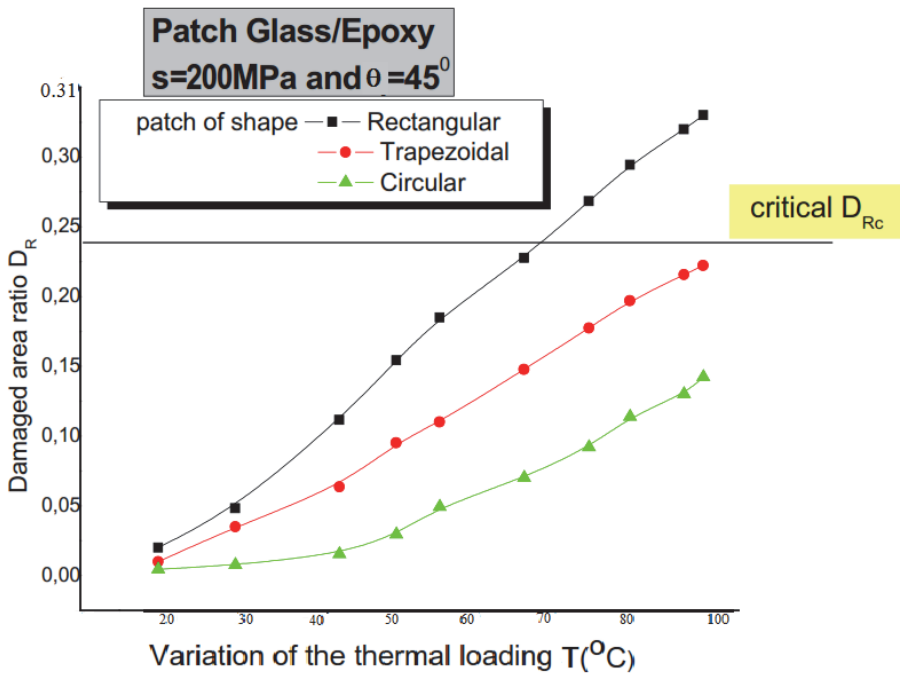


Figure 10: Variation of the damaged zone ratio D_R vs the temperature for the Boron-epoxy type.

Case of the Graphite-epoxy patch. Fig. 11 presents the variation of D_R as a function of the variation in temperature ΔT for a graphite / epoxy type patch and with a crack size $a = 30\text{mm}$ and inclination $\theta =45^{\circ}$. It is noticed that the D_R increases with the increase in the temperature variation ΔT . We can also observe that the rectangular geometric shape is the least efficient for this repair because it gives values of D_R clearly greater than that of the D_{RC} and this as soon as $\Delta T > 55^{\circ}\text{C}$. The best performing shape is circular because the critical value of the damaged area ratio is only reached when $\Delta T > 75^{\circ}\text{C}$.

Case of the Glass-epoxy patch. Fig. 12 shows the variation of the D_R as a function of the temperature variation for a glass / epoxy patch for the three geometric shapes (rectangular, trapezoidal and circular) for the same adhesive (FM 73). The D_R ratio increases with increase in the temperature variation ΔT . One can notice that the circular shape is the best because it gives values of the ratio D_R that are the lowest compared to the other shapes. The results of D_R for the rectangular shape of the patch exceed the critical value $D_{RC} = 0.2475$ when the $\Delta T \approx 65^{\circ}\text{C}$. It can be concluded that this form should be avoided for this type of repair.

Figure 11: Variation of the damaged zone ratio D_R vs the temperature for the Graphite-epoxy type.Figure 12: Variation of the damaged zone ratio D_R vs the temperature ΔT for the Glass-epoxy type.

Variation of stress intensity factor in mixed mode as a function of temperature $\Delta(T)$ for the different types of the patch

The criterion of Von-Mises is used as criterion of plasticity. The theory of additional plasticity is introduced to model the non-linearity of the adhesive material. The stress intensity factors at the crack tip are calculated using the virtual crack closure technique (VCCT) based on the energy balance. In this technique, the stress intensity factors are obtained for the three failure modes according to the equation:

$$G_i = \frac{K_i^2}{E} \quad (5)$$

where G_i is the Fracture energy for mode I, K_i is the stress intensity factor for mode i and E is the modulus of elasticity. The model referred to above is called the linear elastic fracture mechanics model and has found wide acceptance as a method for determining the resistance of a material to below-yield strength fractures. The model is based on the use of linear elastic stress analysis; therefore, in using the model one implicitly assumes that at the initiation of fracture any localized plastic deformation is small and considered within the surrounding elastic stress field.

$$\begin{aligned}\sigma_x &= \frac{K}{\sqrt{2\pi r}} \cos \frac{\theta}{2} \left[1 - \sin \frac{\theta}{2} \sin \frac{30}{2} \right] \\ \sigma_y &= \frac{K}{\sqrt{2\pi r}} \cos \frac{\theta}{2} \left[1 + \sin \frac{\theta}{2} \sin \frac{30}{2} \right] \\ \sigma_{xy} &= \frac{K}{\sqrt{2\pi r}} \sin \frac{\theta}{2} \left[\cos \frac{\theta}{2} \cos \frac{30}{2} \right]\end{aligned}\quad (6)$$

The stress in the third direction are given by $\sigma_z = \sigma_{xz} = \sigma_{yz} = 0$ for the plane stress problem, and when the third directional strains are zero (plane strain problem), the out of plane stresses become $\sigma_{xz} = \sigma_{yz} = 0$ and $\sigma_z = \theta(\sigma_x + \sigma_y)$. While the geometry and loading of a component may change, as long as the crack opens in a direction normal to the crack path, the crack tip stresses are found to be as given by Eqns. 6.

The stress intensity factor (K) is used in fracture mechanics to predict the stress state "stress intensity" near the tip of a crack or notch caused by a remote load or residual stresses. It is a theoretical construct usually applied to a homogeneous, linear elastic material and is useful for providing a failure criterion for brittle materials, and is a critical technique in the discipline of damage tolerance. The concept can also be applied to materials that exhibit small-scale yielding at a crack tip. The magnitude of K depends on specimen geometry, the size and location of the crack or notch, and the magnitude and the distribution of loads on the material. It can be written as [23, 24]:

$$K = \sigma \sqrt{\pi a f \left(\frac{a}{W} \right)} \quad (7)$$

where: $f \left(\frac{a}{W} \right)$ is a specimen geometry dependent function of the crack length a , the specimen width W , and σ is the applied stress.

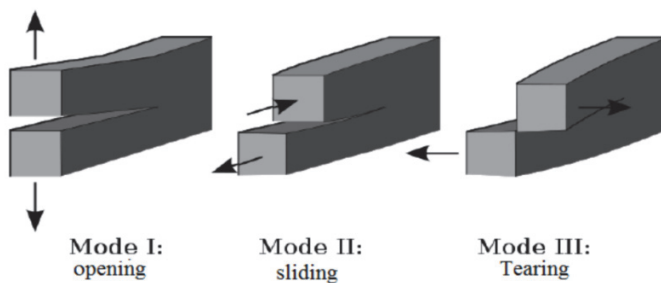


Figure 13: Mode I, Mode II, and Mode III crack loading.

In 1957, G. Irwin found that the stresses around a crack could be expressed in terms of a scaling factor called the stress intensity factor. He found that a crack subjected to any arbitrary loading could be resolved into three types of linearly independent cracking modes.[25] These load types are categorized as Mode I, II, or III as shown in the Fig. 13. Mode I is



an opening (tensile) mode where the crack surfaces move directly apart. Mode II is a sliding (in-plane shear) mode where the crack surfaces slide over one another in a direction perpendicular to the leading edge of the crack. Mode III is a tearing (antiplane shear) mode where the crack surfaces move relative to one another and parallel to the leading edge of the crack. Mode I is the most common load type encountered in engineering design.

Different subscripts are used to designate the stress intensity factor for the three different modes. The stress intensity factor for mode I is designated K_I and applied to the crack opening mode. The mode II stress intensity factor K_{II} , applies to the crack sliding mode and the mode III stress intensity factor K_{III} applies to the tearing mode. These factors are formally defined as [26]:

$$\begin{aligned} K_I &= \lim_{r \rightarrow 0} \sqrt{2\pi r} \sigma_{yy}(r, 0) \\ K_{II} &= \lim_{r \rightarrow 0} \sqrt{2\pi r} \sigma_{yx}(r, 0) \\ K_{III} &= \lim_{r \rightarrow 0} \sqrt{2\pi r} \sigma_{yz}(r, 0) \end{aligned} \quad (8)$$

$$K_I = \alpha \beta \sqrt{\pi a} \quad (9)$$

$$\beta = \left(1 - 0.025\alpha^2 + 0.06\alpha^4\right) \sqrt{\sec \frac{\alpha\pi}{2}}$$

where,

K_I =Stress intensity factor

β = Geometry factor

$\alpha = 2a/W$

$2a$ = Crack length

W = Width of the plate

σ = Force applied

Where the factor β is used to relate gross geometrical features to the stress intensity factor

$$K_I = \sigma \sqrt{\pi a} \left[\frac{1 - \frac{a}{2b} + 0.326 \left(\frac{a}{b} \right)^2}{\sqrt{1 - \frac{a}{b}}} \right] \quad (10)$$

Crack in a finite plate under mode I loading.

The generalized form for mode II stress intensity factor can be expressed as:

The Mode II stress intensity factor K_{II} is derived using the following equation [27],

$$K_{II} = \rho \sqrt{\pi a} (1 - \alpha) \sin \beta \cos \beta \quad (11)$$

The second part of this work shows the effect of temperature on the behavior of the corroded and cracked aluminum plate with an inclined crack in mixed mode (mode I+ mode II). The evolution of the stress intensity factor ($K_I + K_{II}$) for several angles of crack inclination and the three types of composite patch was shown in Fig. 14. The analysis of these curves obtained for the circular shape allows the observation of the effect of the crack inclination. It can be seen that the increase in the angle of the crack inclination leads to a decrease in the values of the sum ($K_I + K_{II}$) for all the types of composite patch used. As for the second observation concerning the type of patch, the values of ($K_I + K_{II}$) obtained for boron/epoxy are better than those of (graphite/epoxy and glass/epoxy). For the angle of inclination $\theta = 30^\circ$ and for $\Delta T = 0^\circ C$ ($T = 20^\circ C$), the value for boron/epoxy of ($K_I + K_{II}$) is $7 \text{ MPa.m}^{1/2}$ but for graphite/epoxy ($K_I + K_{II}$) = $9.75 \text{ MPa.m}^{1/2}$ and for Glass/epoxy the value of ($K_I + K_{II}$) $7.75 \text{ MPa.m}^{1/2}$. Therefore, the following conclusions can be as follows

increasing the angle of the crack inclination leads to a decrease in the values of stress intensity factor (K_I+K_{II}). On the other hand, an increase in the temperature induces an increase in the stress intensity factor (K_I+K_{II}). From the previous results it can be concluded that the boron/epoxy patch is the best because it gives low values of (K_I+K_{II}).

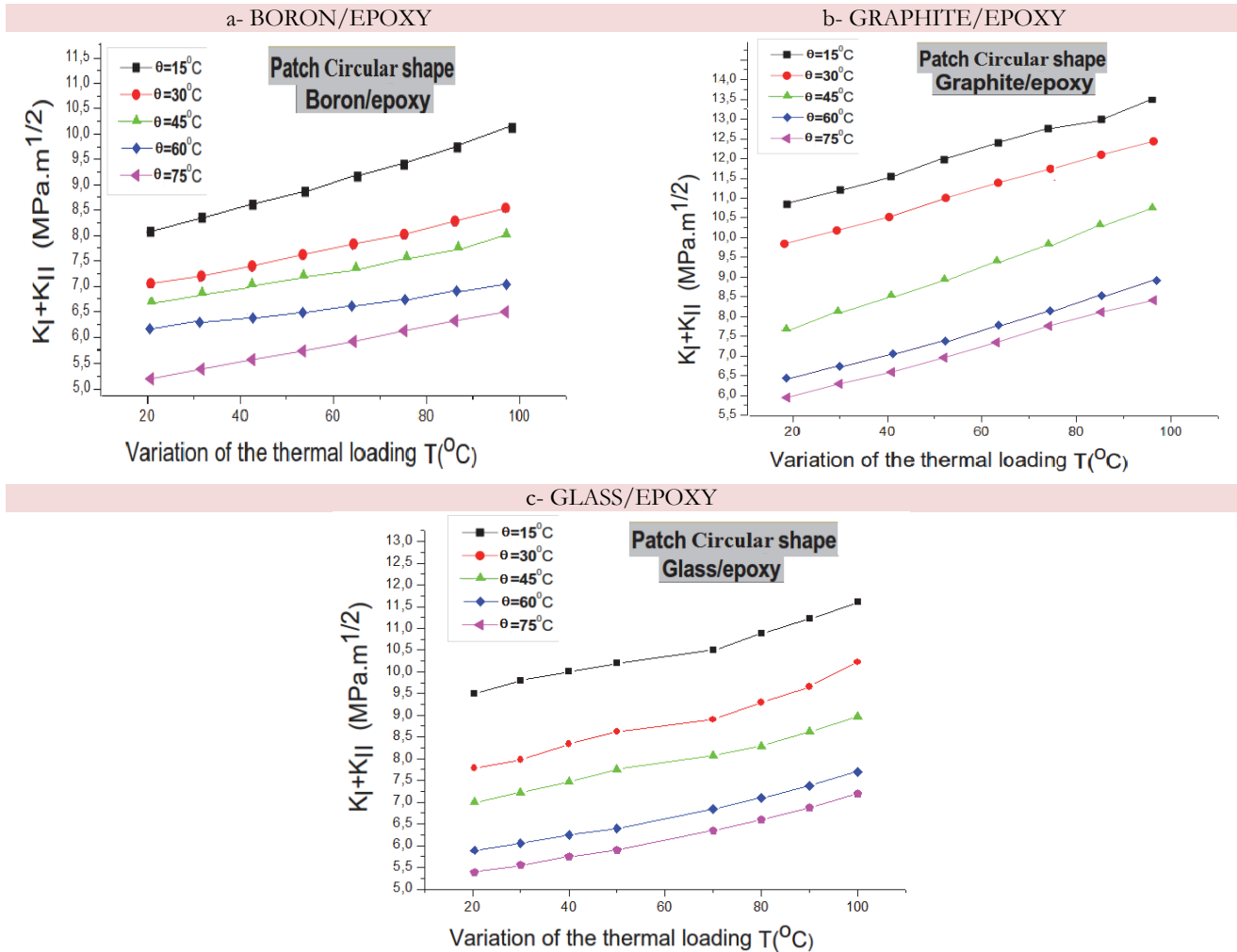


Figure 14: Variation of stress intensity factor (K_I+K_{II}) vs the temperature T for the circular shape. (a) boron/epoxy, (b) graphite/epoxy and (c) glass/epoxy.

GENERAL CONCLUSION

The repair of composite materials is a major challenge for the aeronautic transport industries. The repairs currently used are poorly adapted to low-energy impact damage and are very costly. The purpose of this paper was to study the behavior of a corroded and cracked plate with an inclined crack under thermomechanical loading using the finite element method. This work consists in evaluating the damaged area of the adhesive from several effects under thermal loading. The objective was to calculate the damaged area ratio, determine the stress intensity factor in the mixed mode (K_I+K_{II}) repair by composite patch then compare the results for the different shapes of the patch (rectangular, trapezoidal and circular). The distribution of the damaged areas in the adhesive as well as the stress intensity factor led to the following conclusions.

The effect of crack inclination θ for $\Delta T=0^\circ C$

- For the different shapes of the patch used the value of the D_R decreases with the increase in the crack inclination.

The effect of temperature variation ΔT for $\theta=45^\circ$

- It can be noticed that the more the temperature variation ΔT increases, the more the surface of the damaged area increases for all the shapes of the patch (rectangular, trapezoidal and circular).



- The D_R increases with the increase in the temperature variation ΔT .
- The rectangular shape is to be avoided for the repair because it gives very high values D_R .
- The most efficient shape is the circular shape.
- The increase in the angle of the crack inclination generates a decrease in the stress intensity factor values ($K_I + K_{II}$).
- The increase in temperature leads to an increase in the stress intensity factor ($K_I + K_{II}$).
- The Boron/Epoxy type patch is the best because it gives low values of ($K_I + K_{II}$).

REFERENCES

- [1] Berrahou, M. and Bachir Bouiadra, B.B. (2016). Analysis of the adhesive damage for different patch shapes in bonded composite repair of corroded aluminum plate, *J. Techno. Press.* 59(1), pp. 123-132. DOI: 10.12989/sem.2016.59.1.123.
- [2] Berrahou, M., Salem, M., Mechab, B. and Bachir Bouiadra, B.B. (2017). Effect of the corrosion of plate with double cracks in bonded composite repair, *J. Techno. Press.* 64(1), pp. 323-328. DOI: 10.12989/sem.2017.64.3.323.
- [3] Berrahou, M., Salem, M. and Mechab, B. (2019). Analysis of the plate failure repaired by composite patch and reinforced by stiffeners, 1st Conference on Renewable Energies & Advanced Materials ERMA'19 – Relizane, Algeria. December 16 and 17, pp. 276-280.
- [4] Amari, K., Berrahou, M. and Serier, M. (2019). Numerical analysis of the crack propagation in a notched plate under mechanical loading, 1st Conference on Renewable Energies & Advanced Materials ERMA'19 – Relizane, Algeria. December 16 and 17, pp. 827-833.
- [5] Salem M., Serier, M. and Berrahou, M. (2019). the adhesive Damage of a repaired corroded and cracked plate under mechanical loading, 1st Conference on Renewable Energies & Advanced Materials ERMA'19 – Relizane, Algeria. December 16 and 17, pp.834-840.
- [6] Salem, M., Berrahou, M., Mechab, B. and Bachir Bouiadra, B.B. (2017). Effect of the angles of the cracks of corroded plate in bonded composite repair, *J. Frattura ed Integrità Strutturale.* 46(1), pp. 113-123. DOI: 10.3221/IGF-ESIS.46.12.
- [7] Benyahia, F., Albedah, A. and Bachir Bouiadra, B.B. (2014). Analysis of the adhesive damage for different patch shapes in bonded composite repair of aircraft structures, *J. mat des.* 54, pp. 18-24. DOI: 10.1016/j.matdes.2013.08.024.
- [8] Fari Bouanania, M., Benyahia, F., Albedah, A., Bachir Bouiadra, B.B., Belhouari, M. and Achour, T. (2013). Analysis of the adhesive failure in bonded composite repair of aircraft structures using modified damage zone theory, *J. mat des.* 50, pp. 433-439. DOI: 10.1016/j.matdes.2013.03.017.
- [9] Sadek, K., Bennouna. M.S., Aour, B., Bachir Bouiadra, B.B., Benaissa A. and Fari Bouanani, M. (2019). Numerical Investigation of the Adhesive Damage Used for the Repair of A5083 H11 Aluminum Structures by Composites Patches, *J. International Journal of Engineering Research in Africa.* 44, pp.22-44. DOI: 10.4028/www.scientific.net/JERA.44.22.
- [10] Cheng ye Fana, P.Y., Ben Jara, J.J. and Roger Chengb. (2008). Cohesive zone with continuum damage properties for simulation of delamination development in fibre composites and failure of adhesive joints, *J.eng frac mecanichal.* 75, (13), pp. 3866-3880. DOI: 10.1016/j.engfracmech.2008.02.010.
- [11] Deok-Bo, L., Toru, I., Noriyuki, M. and Nak-Sam, C. (2004). Effect of Bond Thickness on the Fracture Toughness of Adhesive Joints, *J. Eng. Mater. Technol.* 126(1), pp. 14-18. DOI: 10.1115/1.1631433.
- [12] Ibrahim. N.C., Fari Bouanani, M, Bachir Bouiadra, B.B and Serier, B. (2016). Analysis of the adhesive damage between composite and metallic adherends,J. Application to the repair of aircraft structures Advances in Materials Research. 5(1), pp. 11-20. DOI: 10.12989/amr.2016.5.1.011.
- [13] Aminallah, L., Benhamena, Ali., Benaissa, Ali and al. (2014). Numerical analysis of damage evolution in adhesive of bonded composite Material, csc, annaba, Algeria, 9-11 novembre.
- [14] Benyahia, A., Bouanani, F., Bachir Bouiadra, B.B. and Achour, T. (2014). Effect of water absorption on the adhesive damage in bonded composite repair of aircraft structures, *J. mat des.* 57, pp. 435-441. DOI: 10.1016/j.matdes.2013.12.081.
- [15] Rybicki, E.F. and Kanninen, M.F. (1977). A finite element calculation of stress intensity factors by a modified crack closure integral. *Eng. Fract. Mech.* 9(8), 931–938.
- [16] Jokinen, J. and Kanerva, M. (2019). Simulation of Delamination Growth at CFRP-Tungsten Aerospace Laminates Using VCCT and CZM Modelling Techniques, *J. Applied Composite Materials.* 26, pp. 709–721.

- DOI: 10.1007/s10443-018-9746-5.
- [17] Tian, R., Wen, L. and Wang, L. (2018). Three-dimensional improved XFEM (IXFEM) for static crack problems, *J. Comput Methods Appl Mech Eng.* 343, pp.339–367. DOI: 10.1016/j.cma.2018.08.029.
- [18] Bellali, M.A., Mokhtari, M., Benzaama, H., Hamida, F., Serier, B. and Madani, K. (2020). Using CZM and XFEM to predict the damage to aluminum notched plates reinforced with a composite patch, *J Mech Mater Struct.* 15, pp.185–201. DOI: 10.2140/jomms.2020.15.185.
- [19] Raşit, koray Ergün, Hamit, A., Batman, Abdullah, S., Kahramanmaraş, Semsettin, T. (2018). Repair of an aluminum plate with an elliptical hole using a composite patch, *materials testing*, 60 11, pages 1104-1110, DOI: 10.3139/120.015111.
- [20] Salem, M., Berrahou, M., Mechab, B. and Bachir Bouiadra, B.B. (2021). Analysis of the adhesive damage for different patch shapes in bonded composite repair of corroded aluminum plate under thermo-mechanical loading, *j fail. Anal. And preven.* DOI: 10.1007/s11668-021-01167-x
- [21] ABAQUS standard/user's manual, version 6.5. Hibbit Karlsson & Sorensen, Inc., Pawtucket, RI, USA, (2007).
- [22] Ban, C.S., Lee, Y.H., Choi, J.H. and Kweon, J.H. (2008). Strength prediction of adhesive joints using the modified damage zone theory, *J. Compos. Struct.* 86(1), pp. 96-100. DOI: 10.1016/j.compstruct.2008.03.016.
- [23] Soboyejo, W. O. (2003). Crack Driving Force and Concept of Similitude, *J. Mechanical properties of engineered materials*. Marcel Dekker. ISBN 0-8247-8900-8. OCLC 300921090.
- [24] Janssen, M. (2004). Fracture mechanics, Zuidema, J. (Jan), Wanhill, R. J. H. (2nd Ed.). London. Spon Press. p. 41. ISBN 0-203-59686-2. OCLC 57491375.
- [25] Suresh, S. (2004). Fatigue of Materials, Cambridge University Press. ISBN 978-0-521-57046-6.
- [26] Rooke, D. P. and Cartwright, D. J. (1976). Compendium of stress intensity factors, HMSO Ministry of Defence. Procurement Executive.
- [27] Sih, G. C., Paris, P. C. and Erdogan, F. (1962). Crack-tip stress intensity factors for the plane extension and plate bending problem, *Journal of Applied Mechanics*, 29, pp. 306–312, DOI: 10.1115/1.3640546